Pedestrian Navigation in Harsh Environments using Wireless and Inertial Measurements

J. Prieto*, *Member, IEEE,* S. Mazuelas**, *Member, IEEE,*
A. Bahillo*, P. Fernández*, R. M. Lorenzo* and E. J. Abril*
*Department of Signal Theory and Communications and Telematic Engineering, University of Valladolid.
Paseo de Belén 15. 47011. Valladolid. SPAIN. Email: javier.prieto@uva.es
**Laboratory for Information and Decision Systems (LIDS), Massachusetts Institute of Technology,
77 Massachusetts Avenue, Cambridge, MA. 02139. USA. Email: mazuelas@mit.edu

***Abstract*—The popularity of positioning satellite systems in open areas has led to a high demand for systems suitable for harsh environments, where the former fail. Wireless localization and inertial navigation have emerged as the most valuable alternatives to offer positioning in such environments. However, the characteristics of the wireless propagation channel in harsh environments are dynamic and unpredictable while the errors in inertial navigation rapidly increase with time. In this paper, we present a general framework and algorithms for data fusion in navigation systems. The presented techniques combine both wireless and inertial measurements. To assess the proposed methods, we collected measurements from commercial wireless devices and low-cost inertial sensors in a real indoor environment. The experimental results show the remarkable performance of the proposed method, capable of reaching a sub-meter accuracy.**

I. Introduction

The outstanding performance of Global Navigation Satellite Systems (GNSS) in open areas has boosted the development of a wide range of localization based services [1]. At the same time, it has motivated an increasing research interest for positioning alternatives in dense cluttered scenarios, such as indoor or deep urban areas, where GNSS is not operative [2], [3]. Coarsely, these alternatives can be classified as wireless localization and inertial navigation [2], [4].

Wireless localization has been subject to intense interest in the research community, mainly due to the proliferation of wireless local area networks (WLANs). Wireless localization techniques determine the position of a mobile target from measurements taken on the signals transmitted by the nodes in the wireless network [3]–[9]. Most common approaches infer positions from range-related information provided by received signal-strength (RSS) [7] or time-of-arrival (TOA) [8] measurements. Then, the position is estimated by means of a process known as trilateration [3]. The performance of such techniques falls down drastically in environments with severe non-line-of-sight (NLOS) and multipath propagation conditions, such as factories with metal coatings or mines [10]. Several techniques have been developed to address the complex behavior of measurements in harsh wireless environments [4]–[6]. However, either they are far from a sub-meter accuracy or the involved cost precludes a widespread usage.

Inertial navigation is becoming increasingly popular, especially after the irruption of microelectromechanical systems (MEMS)-based inertial measurement units (IMUs). Inertial navigation systems determine the position and orientation of a mobile target from measurements taken by an IMU installed on the target [11]–[18]. Most common approaches infer position and orientation from information related to acceleration and angular velocity provided by accelerometers and gyroscopes, respectively. Then, the position and orientation are obtained by means of numerical integration given their known initial values. Integration carried out from biased measurements derives in a drift in position and orientation that is accumulated with time [11], [12]. Several methods have been developed to address the drift problem with zero-velocity updates (ZUPTs) when they detect stationary stance phases [11]–[18]. However, although more slowly, the systematic errors (bias) introduced by the sensors result in drifts that increasingly disrupt the estimated position and orientation [11], [12].

Strengths and weaknesses of both, wireless localization and inertial navigation, have inevitably focused the challenge for researchers in developing systems that couple wireless and inertial measurements without substantially increasing complexity and cost [2], [19]. Several approaches have dealt with the hybrid challenge in harsh environments: low-power radar and radio-frequency sensors are used, respectively, for ZUPT in [15] and [16]; wireless-aided inertial navigation is proposed but not implemented in [17] together with human-controlled map-matching; RSS-assisted ZUPT is implemented in [14]; whereas in [18] map and WLAN information aids a localization particle filter to constrain the position estimates achieved by a ZUPT-based Kalman-like navigation system.

In this paper, we propose a framework for pedestrian navigation based on Bayesian data fusion. Such framework addresses the mentioned drawbacks by incorporating measurements coming from wireless devices and inertial sensors. In order to show the performance improvement achieved, we assess this framework with measurements collected by low-cost MEMS-IMUs and commercial WLAN devices in a real indoor scenario.

This research is partially supported by the Directorate General of Telecommunications of the Regional Ministry of Public Works and the Regional Ministry of Education from Castilla y León (Spain), by the Spanish national project LORIS (TIN2012-38080-C04-03) and by the European Social Fund.

The paper is organized as follows: Section II states the problem and defines the random variables involved in the estimation; Section III presents the framework for pedestrian navigation based on data fusion of wireless and inertial measurements; Section IV assesses the proposed scheme by means of several experimental probes; and finally, Section V summarizes the conclusions drawn from the research.

II. Problem Statement

In this section, we formulate the problem of estimating the position of a mobile target in a three-dimensional scenario by fusing information from both wireless devices and inertial sensors. In order to do that, we collect measurements, $\{\mathbf{z}_k\}_{k\in\mathbb{N}}$, at discrete time instants, $t_{k\in\mathbb{N}}$. From these measurements, we estimate the state vector, $\{\mathbf{y}_k\}_{k\in\mathbb{N}}$. In the following, we define the entries to both measurements and state vectors.

The measurements vector $\mathbf{z}_k = [\mathbf{z}_k^{\mathbf{f}\,T}, \mathbf{z}_k^{\boldsymbol{\omega}\,T}, \mathbf{z}_k^{s\,T}, \mathbf{z}_k^{\tau\,T}]^T$, where $\mathbf{z}_k^{\mathbf{f}} \in \mathbb{R}^3$ are the specific force measurements from the accelerometers, $\mathbf{z}_k^{\boldsymbol{\omega}} \in \mathbb{R}^3$ the angular velocity measurements from the gyroscopes, $\mathbf{z}_k^s \in \mathbb{R}^{L^s}$ the RSS measurements with respect to L^s anchors, and $\mathbf{z}_k^\tau \in \mathbb{R}^{L^\tau}$ the TOA measurements with respect to L^τ anchors.[1]

The state vector $\mathbf{y}_k = [\mathbf{x}_k^T, \mathbf{v}_k^T, \mathbf{a}_k^T, \bar{q}_k^T, \boldsymbol{\omega}_k^T, \boldsymbol{\Theta}_k^T]^T$, where $\mathbf{x}_k \in \mathbb{R}^3$ is the mobile target's position, $\mathbf{v}_k \in \mathbb{R}^3$ its velocity, $\mathbf{a}_k \in \mathbb{R}^3$ its acceleration, $\bar{q}_k \in \mathbb{H}$ its orientation, and $\boldsymbol{\omega}_k \in \mathbb{R}^3$ its angular velocity, all of them represented in the navigation reference frame. The set $\boldsymbol{\Theta}_k \in \mathbb{R}^6$ includes biases in the measurements collected by the accelerometers, $\mathbf{b}_k^{\mathbf{f}} \in \mathbb{R}^3$, and the gyroscopes, $\mathbf{b}_k^{\boldsymbol{\omega}} \in \mathbb{R}^3$.

In the previously defined state vector, we include derivatives of position until acceleration since it relates the specific force measurements from the IMU and the desired target's position. Moreover, in an inertial navigation system, IMUs provide measurements in their own body reference frame whereas the aim is to obtain the position in the navigation reference frame. Therefore, the state vector also includes the rotation from the navigation frame to the body frame, referred in this paper as orientation. As a consequence, we include the angular velocity in the state vector since it relates the gyroscope measurements from the IMU and the desired sensor's orientation.

With respect to the orientation, we select the unit quaternion, $\bar{q}_k \in \mathbb{H}$, for its representation, i.e., $\bar{q}_k$ is the rotation from the navigation frame to the sensor body frame. Although we can select different representations that range from minimal three-dimensional vectors to nine-element rotation matrices [20], four-dimensional quaternions are the preferred representation for real-time navigation systems. Regarding minimal three-dimensional vectors, some of them impose constraints in the models (such is the case of Euler angles) whereas other vectors present singularities in their dynamic or measurements models (such as the rotation vector governed by Bortz's equation [21]). On the other hand, rotation matrices have little use owing to their high dimension and constraints imposed to the dynamic model [20]. Finally, unit quaternions offer a nonsingular parametrization with a rather simple dynamic model [22].[2] The unit quaternion is defined as,

$$\bar{q}_k = \begin{bmatrix} \cos(\frac{\|\mathbf{u}_k\|}{2}) \\ \frac{\mathbf{u}_k}{\|\mathbf{u}_k\|}\sin(\frac{\|\mathbf{u}_k\|}{2}) \end{bmatrix},$$

based on the idea that the orientation can be defined by an axis $\mathbf{u}_k$ and the angle of rotation $\|\mathbf{u}_k\|$.

With the defined measurements and state vectors, it can be assumed that given the current state vector, $\mathbf{y}_k$, the measurements vector, $\mathbf{z}_k$, is independent of all previous and future states and measurements [24]. Therefore, we can build a hidden Markov model that leads to two kinds of dependence between the random variables: the relationship between the state vector in time t_k and the state vector in time t_{k-1}, i.e., $p(\mathbf{y}_k|\mathbf{y}_{k-1})$, called *dynamic model*; and the relationship between the measurements and the state vector in each time, i.e., $p(\mathbf{z}_k|\mathbf{y}_k)$, called *measurements model* [5], [24]. Next sections derive both dynamic and measurements models utilized for the estimation of the state vector in the navigation system.

III. Navigation Framework

Since the problem of estimating positions from wireless and inertial measurements is addressed from a Bayesian perspective, the key elements to perform the estimation are the dynamic and measurements models that we present afterwards [24], [25].

A. Dynamic Model

Given $\mathbf{x}_k$, $\mathbf{v}_k$ and $\mathbf{a}_k$, we can approximate their values in time t_{k+1} by means of their Taylor series expansion as,

$$\begin{bmatrix} \mathbf{x}_{k+1} \\ \mathbf{v}_{k+1} \\ \mathbf{a}_{k+1} \end{bmatrix} = \begin{pmatrix} 1 & \Delta_k & \frac{\Delta_k^2}{2} \\ 0 & 1 & \Delta_k \\ 0 & 0 & 1 \end{pmatrix} \begin{bmatrix} \mathbf{x}_k \\ \mathbf{v}_k \\ \mathbf{a}_k \end{bmatrix} + \mathbf{n}_k^{d,1}, \qquad (1)$$

where $\Delta_k = (t_{k+1} - t_k) \in \mathbb{R}$ is the sampling interval, and $\mathbf{n}_k^{d,1} \in \mathbb{R}^9$ is the error term that can be modeled as a random variable, where the most common is to model it as white Gaussian noise (i.e. a discrete Wiener process) [24].

With the election of the quaternion $\bar{q}_k$ as representation of the orientation, the differential equation that relates it to the angular velocity is given by [26],

$$\frac{\partial}{\partial t}\bar{q}(t) = -\frac{1}{2}\bar{\omega}(t) \odot \bar{q}(t), \qquad (2)$$

where $\bar{\omega}(t) = [0, \boldsymbol{\omega}(t)^T]^T$ is the unit quaternion corresponding to the angular velocity, and the operator $\odot$ indicates the quaternion multiplication defined according to the Appendix.[3] Since MEMS-based IMUs provide measurements at frequencies around 100 Hz, we can assume that the direction of $\boldsymbol{\omega}(t)$

[1] In each time instant, we receive at least one of those measurements types, not being necessary to receive all of them at the same time.

[2] Since the quaternion has four components, it presents an additional degree of freedom in comparison to three-dimensional representations [23]. Hence, its module has to be normalized after each iteration.

[3] The change of sign in (2) reflects the fact that the orientation represents the rotation from the navigation frame to the sensor body frame, whereas the gyroscope provides measurements in the opposite sense.

is constant during the time interval between two measurements [27]. Hence, we can formally integrate (2) and model the change in orientation as [28],

$$\bar{q}_{k+1} = \exp(-\frac{1}{2}\bar{\omega}_k) \odot \bar{q}_k + \bar{n}_k^{d,2}, \tag{3}$$

where the error term, $\bar{n}_k^{d,2} \in \mathbb{H}$, can be assumed to be white Gaussian noise.[4]

Regarding the angular velocity and the biases, we consider a random walk as dynamic model, that is,

$$\begin{bmatrix} \boldsymbol{\omega}_{k+1} \\ \boldsymbol{\Theta}_{k+1} \end{bmatrix} = \begin{bmatrix} \boldsymbol{\omega}_k \\ \boldsymbol{\Theta}_k \end{bmatrix} + \mathbf{n}_k^{d,3}, \tag{4}$$

where the error $\mathbf{n}_k^{d,3} \in \mathbb{R}^9$ is modeled as white Gaussian noise.

In summary, the whole dynamic model is given by (1), (3) and (4), which is non-linear and Gaussian.

B. Measurements Model

In the following, we describe realistic models for the relationship between both wireless and inertial measurements and the state vector, for dense cluttered environments.

The range-related information comes from RSS and TOA measurements taken on the wireless signals, which are the metrics that hold promise to obtain the performance needed with an appropriate system complexity and cost [5].

The RSS values are influenced, among other factors, by the distance between target and anchors. This attenuation is proportional to the inverse of the distance raised to a path-loss exponent [7], [9]. By isolating this dependence in logarithmic units we have,

$$z_k^s = \alpha^s - 10\beta^s \log_{10}(\|\mathbf{x}^l - \mathbf{x}_k\|) + n_k^s, \tag{5}$$

where $\mathbf{x}^l \in \mathbb{R}^3$ is the position of the lth anchor, $\alpha^s \in \mathbb{R}$ is a constant that depends on several factors such as fast and slow fading, gains in transmitter and receiver antennas and the transmitted power, and $\beta^s \in \mathbb{R}$ is the path-loss exponent [7]. Finally, n_k^s is a noise term caused by shadowing where this random variable has zero mean in cases where the parameters α^s and β^s fit perfectly the current propagation conditions [7], [9]. In practice, the value of α^s can be previously known. However, in realistic scenarios, the path loss exponent, β^s, does not fit exactly the actual propagation conditions, and hence, the noise term, n_k^s, has a non-zero mean proportional to the logarithm of the distance.

The TOA measurements regarding a given anchor are related to the target's position at time t_k by,[5]

$$z_k^\tau = \alpha^\tau + \beta^\tau \|\mathbf{x}^l - \mathbf{x}_k\| + n_k^\tau, \tag{6}$$

being $\alpha^\tau \in \mathbb{R}$ and $\beta^\tau \in \mathbb{R}$ constants that can be previously obtained [29], [30]. The term $n_k^\tau \in \mathbb{R}$ is white Gaussian noise in cases of line-of-sight (LOS) propagation. However, several distributions have been selected to model this error in cases of NLOS propagation, such as Gaussian, Exponential, Rayleigh, Weibull or Gamma [9], [31].

The accelerometer integrated in the IMU provides specific force measurements in the sensor body frame, $\mathbf{z}_k^\mathbf{f} \in \mathbb{R}^3$ [13]. However, we are interested in knowing the acceleration in the navigation frame, $\mathbf{a}_k$. The relationship between both magnitudes is given by,[6]

$$\begin{aligned} \mathbf{z}_k^\mathbf{f} &= \mathbf{f}_k + \mathbf{b}_k^\mathbf{f} + \mathbf{n}_k^\mathbf{f} \\ &= \mathbf{C}(\bar{q}_k)(\mathbf{a}_k - \mathbf{g}) + \mathbf{b}_k^\mathbf{f} + \mathbf{n}_k^\mathbf{f}, \end{aligned} \tag{7}$$

where $\mathbf{f}_k \in \mathbb{R}^3$ is the force in the sensor body frame, $\mathbf{g} \in \mathbb{R}^3$ is the gravity, and $\mathbf{C}(\bar{q}_k) \in \mathbb{R}^{3\times3}$ is the rotation matrix, which represents the same rotation as the unit quaternion $\bar{q}_k$ and is obtained as shown in the Appendix. The error term, $\mathbf{n}_k^\mathbf{f} \in \mathbb{R}^3$, accounts for the random error, white Gaussian, and $\mathbf{b}_k^\mathbf{f} \in \mathbb{R}^3$ is the systematic error (bias) introduced in the specific force measurements by the sensor.

The gyroscope included in the IMU collects angular velocity measurements related to the state by

$$\mathbf{z}_k^{\boldsymbol{\omega}} = \boldsymbol{\omega}_k + \mathbf{b}_k^{\boldsymbol{\omega}} + \mathbf{n}_k^{\boldsymbol{\omega}}, \tag{8}$$

where $\mathbf{n}_k^{\boldsymbol{\omega}} \in \mathbb{R}^3$ is white Gaussian noise and $\mathbf{b}_k^{\boldsymbol{\omega}} \in \mathbb{R}^3$ are the systematic errors introduced by the sensor.

In summary, the whole measurements model is given by (5), (6), (7) and (8), which is non-linear and non-Gaussian.

C. Heuristic Bias Correction

As mentioned above, methods that rely on ZUPTs achieve significant improvements in pedestrian tracking [11]–[18]. Following the same philosophy, we add to our framework evidences of zero velocity, acceleration and angular velocity when a stance phase of the target is detected.

To detect these stance phases we implement the multicondition algorithm proposed by Jiménez *et al*. in [33]. This algorithm establishes three logical conditions that must be satisfied by the measurements collected by the foot-mounted IMU itself (both from accelerometers and gyroscopes). Specifically, the conditions are imposed to the magnitude and variance of the specific force and the magnitude of the angular velocity. Afterwards, the algorithm applies a logical "AND" to those conditions and introduces the result in a median filter. When the output of the filter is a logical "1" the foot is assumed to be stationary. In such a case, we introduce the evidence of zero velocity, acceleration and angular velocity in our navigation framework. The measurements model for this evidence is,

$$\mathbf{0} = \begin{bmatrix} \mathbf{v}_k \\ \mathbf{a}_k \\ \boldsymbol{\omega}_k \end{bmatrix} + \mathbf{n}_k^\mathbf{0}, \tag{9}$$

where $\mathbf{0} \in \mathbb{R}^9$ correspond to the velocity, acceleration and angular velocity evidences, and $\mathbf{n}_k^\mathbf{0} \in \mathbb{R}^9$ can be modeled as white Gaussian noise.

In summary, the measurements model for the evidences of stance phases is given by (9), which is linear and Gaussian.

[4]The quaternion exponential function is defined in the Appendix.

[5]We consider wireless signals with constant speed in a homogeneous media, such as electromagnetic waves in the air. The intercept term in (6), α^τ, is non-zero when TOA is measured through round-trip time techniques [29].

[6]We consider that the region of interest is small enough to assume the Earth's rotation negligible and the gravity constant [32].

IV. Results

The goal of this section is to quantify the performance of the navigation framework described in the above sections. In order to do that, we obtained experimental data in a real indoor scenario and ran several Monte Carlo simulations. In the following, we describe the set-up for the experiments and present the performance results.

A. Experimental Set-up

To obtain the navigation results we utilized the dynamic and measurements models described in Section III. The complexity constraints imposed by a real-time navigation system led to the election of a Kalman-like solution [25]. The lack of linearity in the models of Section III implies the usage of a suboptimal solution, where the most common is to use the extended Kalman filter (EKF). However, we selected the unscented Kalman filter (UKF) since it better captures the higher order moments caused by the non-linear transformation and avoids the computation of Jacobian and Hessian matrices [34].

The mobile target was a pedestrian that covered the path shown in Fig. 1, completing eight laps to the route. The total length of the path is approximately 915 meters, implying a total time of 16 minutes.

Concerning the dynamic model, we selected as standard deviation $\sigma_{d^{(3)}} = 4.5 \cdot 10^2$ m/s^3 for the error regarding position and its derivatives, $\sigma_{\bar{q}'} = 10^{-4}$ /s for the error in the orientation approximation, $\sigma_{\boldsymbol{\omega}'} = 10$ rad/s^2 for the error related to the angular velocity, and $\sigma_{b^{\mathbf{f}}} = 13.5 \cdot 10^{-2}$ m/s^2 and $\sigma_{b^{\boldsymbol{\omega}}} = 6 \cdot 10^{-4}$ rad/s for the bias in specific force and angular velocity measurements, respectively. All of these values are roughly 50% of the maximum [24].

Inertial measurements were performed by using the XSens MTx IMU based on MEMS technology, working at a frequency of 100 Hz ($\Delta_k = 0.01$ seconds). These measurements are considerably affected by the inherent bias of MEMS technology. The values for the covariance matrices of the errors in the inertial measurements were obtained from the manufacture specifications.

RSS and TOA measurements were collected by using the 802.11 systems described in [7] and [8], respectively, receiving a set of 50 measurements of each type with respect to 4 access points (APs) at intervals of approximately 1 second. These measurements are considerably affected by the NLOS and multipath propagation conditions. The values for the covariance matrices of the errors in the wireless measurements were selected based on previous works [5], [7], [8].

Relating to the evidences of stance phases, we set as standard deviation $\sigma_{\mathbf{v}^{\mathbf{o}}} = 10^{-2}$ m/s for the zero-velocity evidences, $\sigma_{\mathbf{a}^{\mathbf{o}}} = 3 \cdot 10^{-1}$ m/s^2 for the zero-acceleration evidences, and $\sigma_{\boldsymbol{\omega}^{\mathbf{o}}} = 5 \cdot 10^{-2}$ rad/s for the zero-angular velocity evidences.

B. Assessment with Actual Measurements

This section reflects the improvement achieved by means of the proposed framework for data fusion in comparison to the individual results of wireless localization and inertial navigation. Table I and Figs. 1 and 2 summarize the results for the selected UKF and for the EKF commonly used. For these results, we call,

- EKF-WiFi, UKF-WiFi: the positions obtained by means of an EKF and an UKF, respectively, by only fusing RSS and TOA measurements.
- EKF-IMU, UKF-IMU: the positions obtained by means of an EKF and an UKF, respectively, by exclusively using inertial measurements and evidences of stance phases.
- EKF-Fusion, UKF-Fusion: the positions obtained by means of an EKF and an UKF, respectively, by implementing the whole described framework that fuses wireless and inertial measurements, as well as evidences of stance phases.

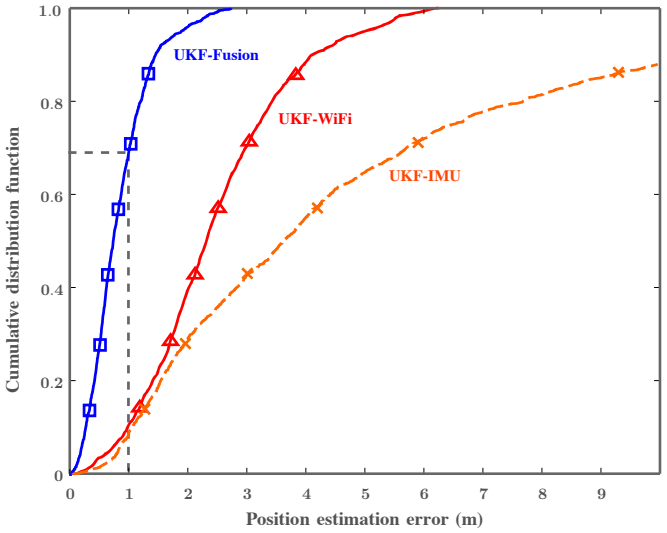

Figure 2. The proposed navigation algorithm achieves an error lower than 1 m for 70% of the positions, and lower than 3 m for all of them.

Table I summarizes for all these methods the quartiles of the error in position estimates as well as the root-mean-square error (RMSE). All these statistics are shown for three different number of laps in order to study the influence of the drift in the final performance.

Figure 2 depicts the cumulative distribution function of the error in position estimation after applying UKF-WiFi, UKF-IMU and UKF-Fusion methods. This figure shows the errors obtained after completing the eight laps to the route.

From Table I and Figs. 1 and 2, we can point out that 1) UKF obtains at least the same performance as EKF with a similar complexity and easier implementation, 2) the RMSE in wireless localization remains approximately constant around 2.80 meters, 3) the RMSE in inertial navigation grows with time representing 1.15 %, 0.59 % and 0.67 % of the covered distance for 1, 4 and 8 laps, respectively, and 4) the fusion of wireless and inertial measurements produces a reduction of 65 % in the RMSE, being this error approximately constant and lower than 1 m after covering a distance of 900 meters.

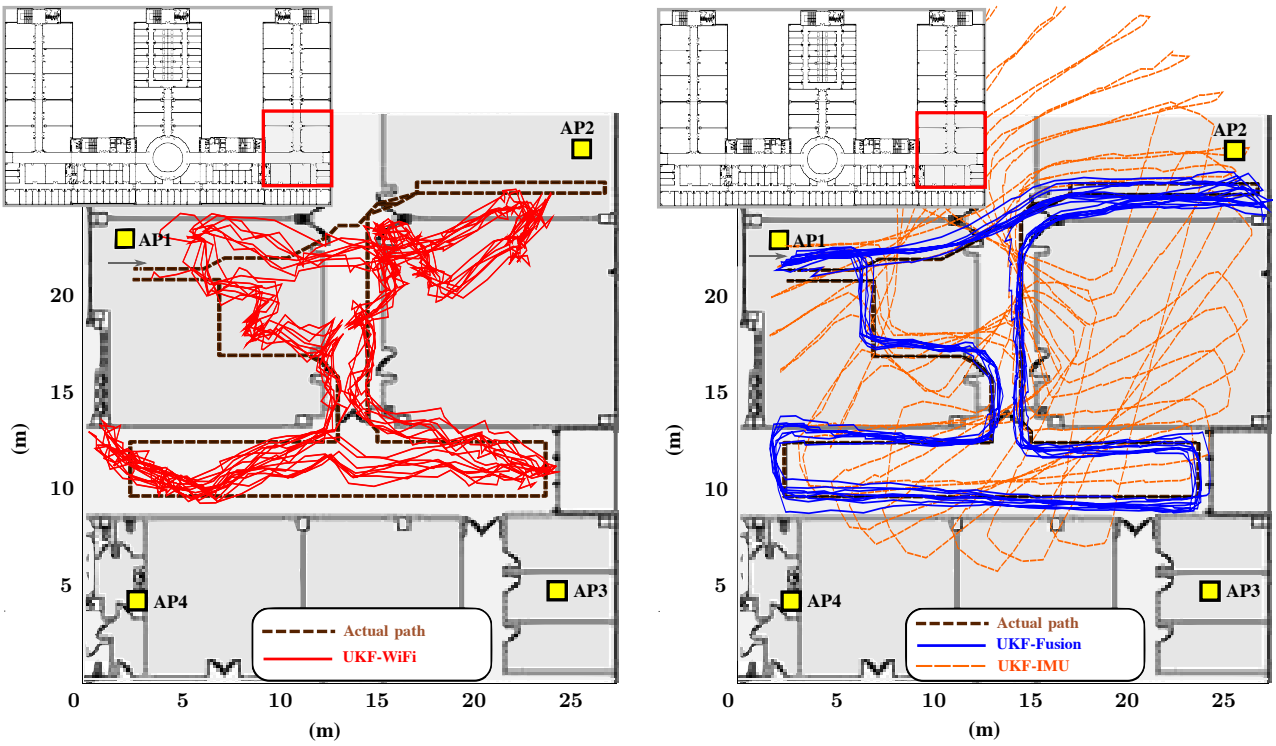

(a) Wireless localization

(b) Navigation (inertial and fusion)

Figure 1. The error in wireless localization is constant but the accuracy is low; the error in inertial navigation grows rapidly with time despite the accurate measurements used; the error after wireless and inertial data fusion is constant, resulting in a very high (sub-meter) accuracy.

Table I
POSITION ESTIMATION ERROR QUARTILES AND RMSE OBTAINED FOR WIRELESS LOCALIZATION, INERTIAL NAVIGATION AND THEIR FUSION, AS A FUNCTION OF THE NUMBER OF LAPS. ALL ERROR VALUES ARE IN METERS.

	1 lap		4 laps		8 laps	
	Quartiles	RMSE	Quartiles	RMSE	Quartiles	RMSE
EKF-WiFi	1.74-2.94-3.60	3.19	1.88-2.75-3.53	3.14	1.96-2.78-3.57	3.17
EKF-IMU	0.65-1.02-1.40	1.17	0.94-1.51-2.54	2.30	1.43-3.20-6.86	6.27
EKF-Fusion	0.48-0.75-1.10	1.00	0.52-0.77-1.12	0.99	0.54-0.79-1.15	1.01
UKF-WiFi	1.58-2.51-3.16	2.83	1.55-2.32-3.13	2.76	1.63-2.34-3.22	2.79
UKF-IMU	0.86-1.13-1.58	1.32	1.29-1.91-3.02	2.69	1.83-3.68-6.57	6.13
UKF-Fusion	0.48-0.76-1.09	1.01	0.47-0.75-1.09	0.98	0.49-0.76-1.12	0.99

V. CONCLUSION

This paper has presented a framework for data fusion in pedestrian navigation systems that exhibits the following advantages concerning previous works: 1) it fuses data coming from wireless and inertial measurements, being extensible to any other kind of measurement; 2) it does not assume a fixed statistical model for the error in the measurements, being possible to particularize the framework as a function of the selected distribution; 3) it incorporates evidences of stationary stance phases, treated as measurements within the framework.

We implemented the proposed framework by means of an UKF, obtaining a remarkable performance as corroborated by measurements collected with a conventional MEMS-IMU and commercial WLAN devices in a harsh environment. Under NLOS and multipath conditions, the mentioned framework obtains a constant RMSE in position estimation, being lower than 1 meter along the whole 900-meters-long path.

REFERENCES

[1] A. Küpper, *Location-Based Services: Fundamentals and Operation*. Chichester, UK: John Wiley & Sons, 2005.

[2] C. Fischer and H. Gellersen, "Location and Navigation Support for Emergency Responders: A Survey," *IEEE Pervasive Computing*, vol. 9, no. 1, pp. 38–47, Jan. 2010.

[3] F. Gustafsson and F. Gunnarsson, "Mobile Positioning Using Wireless Networks," *IEEE Signal Processing Magazine*, vol. 22, no. 4, pp. 41–53, Jul. 2005.

[4] M. Z. Win, A. Conti, S. Mazuelas, Y. Shen, W. M. Gifford, D. Dardari, and M. Chiani, "Network Localization and Navigation via Cooperation," *IEEE Communications Magazine*, vol. 49, no. 5, pp. 56–62, May 2011.

[5] J. Prieto, S. Mazuelas, A. Bahillo, P. Fernández, R. M. Lorenzo, and E. J. Abril, "Adaptive Data Fusion for Wireless Localization in Harsh Environments," *IEEE Transactions on Signal Processing*, vol. 60, Apr. 2012.

[6] A. Kushki, K. Plataniotis, and A. Venetsanopoulos, "Intelligent Dynamic Radio Tracking in Indoor Wireless Local Area Networks," *IEEE Transactions on Mobile Computing*, vol. 9, no. 3, pp. 405–419, Mar. 2010.

[7] S. Mazuelas, A. Bahillo, R. M. Lorenzo, P. Fernández, F. A. Lago, E. García, J. Blas, and E. J. Abril, "Robust Indoor Positioning Provided by Real-Time RSSI Values in Unmodified WLAN Networks," *IEEE*

Journal of Selected Topics in Signal Processing, vol. 3, no. 5, pp. 821–831, Oct. 2009.

[8] A. Bahillo, J. Prieto, S. Mazuelas, R. M. Lorenzo, J. Blas, and P. Fernández, "IEEE 802.11 Distance Estimation based on RTS/CTS Two-Frame Exchange Mechanism," in *IEEE Vehicular Technology Conference*, Apr. 2009.

[9] Y. Qi, "Analysis of Wireless Geolocation in a Non-Line-of-Sight Environment," *IEEE Transactions on Wireless Communications*, vol. 5, no. 3, pp. 672–681, Mar. 2006.

[10] M. Boutin, A. Benzakour, C. L. Despins, and S. Affes, "Radio Wave Characterization and Modeling in Underground Mine Tunnels," *IEEE Transactions on Antennas and Propagation*, vol. 56, pp. 540–549, Feb. 2008.

[11] E. Foxlin, "Pedestrian Tracking with Shoe-Mounted Inertial Sensors," *IEEE Computer Graphics and Applications*, vol. 25, no. 6, pp. 38–46, Nov. 2005.

[12] L. Ojeda and J. Borenstein, "Non-GPS Navigation for Security Personnel and First Responders," *Journal of Navigation*, vol. 60, no. 03, pp. 391–407, Sep. 2007.

[13] D. H. Titterton and J. L. Weston, *Strapdown Inertial Navigation Technology*, 2nd ed. Stevenage: Institution of Engineering and Technology, 2004.

[14] A. R. Jiménez, F. Seco, J. C. Prieto, and J. I. Guevara, "Accurate Pedestrian Indoor Navigation by Tightly Coupling Foot-Mounted IMU and RFID Measurements," *IEEE Transactions on Instrumentation and Measurement*, vol. 61, no. 1, pp. 178–189, Jan. 2012.

[15] C. Zhou, J. Downey, D. Stancil, and T. Mukherjee, "A Low-Power Shoe-Embedded Radar for Aiding Pedestrian Inertial Navigation," *IEEE Transactions on Microwave Theory and Techniques*, vol. 58, no. 10, pp. 2521–2528, Oct. 2010.

[16] C. Zhou, J. Downey, J. Choi, D. Stancil, J. Paramesh, and T. Mukherjee, "A Shoe-Embedded RF Sensor for Motion Detection," *IEEE Microwave and Wireless Components Letters*, vol. 21, no. 3, pp. 169–171, Mar. 2011.

[17] L. Fang, P. J. Antsaklis, L. A. Montestruque, M. B. McMickell, M. Lemmon, Y. Sun, H. Fang, I. Koutroulis, M. Haenggi, M. Xie, and X. Xie, "Design of a Wireless Assisted Pedestrian Dead Reckoning System - The NavMote Experience," *IEEE Transactions on Instrumentation and Measurement*, vol. 54, no. 6, pp. 2342–2358, Dec. 2005.

[18] O. J. Woodman, "Pedestrian Localisation for Indoor Environments," Ph.D. dissertation, University of Cambridge, Sep. 2009.

[19] P. D. Groves, *Principles of GNSS, Inertial, and Multisensor Integrated Navigation Systems*. Artech House, 2008.

[20] M. D. Shuster, "A Survey of Attitude Representations," *The Journal of the Astronautical Sciences*, vol. 41, no. 4, pp. 439–517, Oct. 1993.

[21] J. Bortz, "A New Mathematical Formulation for Strapdown Inertial Navigation," *IEEE Transactions on Aerospace and Electronic Systems*, vol. AES-7, no. 1, pp. 61–66, Jan. 1971.

[22] E. Lefferts, F. Markley, and M. Shuster, "Kalman Filtering for Spacecraft Attitude Estimation," *Journal of Guidance, Control and Dynamics*, vol. 5, pp. 417–429, Sep. 1982.

[23] J. S. Goddard, "Pose and Motion Estimation from Vision Using Dual Quaternion-based Extended Kalman Filtering," Ph.D. dissertation, University of Tennessee, Knoxville, TN, USA, Dec. 1997.

[24] Y. Bar-Shalom, X. R. Li, and T. Kirubarajan, *Estimation with Applications to Tracking and Navigation: Theory Algorithms and Software*. New York: John Wiley & Sons, 2001.

[25] B. Ristic, S. Arulampalam, and N. Gordon, *Beyond the Kalman Filter. Particle Filters for Tracking Applications*. Boston: Artech House Publishers, 2004.

[26] B. Friedland, "Analysis Strapdown Navigation Using Quaternions," *IEEE Transactions on Aerospace and Electronic Systems*, vol. AES-14, no. 5, pp. 764–768, Sep. 1978.

[27] Y. Wu, "A Critique on "On Finite Rotations and the Noncommutativity Rate Vector"," *IEEE Transactions on Aerospace and Electronic Systems*, vol. 48, no. 2, pp. 1846–1847, Apr. 2012.

[28] J. R. Wertz, *Spacecraft Attitude Determination and Control*. Dordrecht: Kluwer Academic Publishers, 1978.

[29] A. Bahillo, S. Mazuelas, R. M. Lorenzo, P. Fernández, J. Prieto, R. J. Durán, and E. J. Abril, "Accurate and Integrated Localization System for Indoor Environments based on IEEE 802.11 Round-Trip Time Measurements," *EURASIP Journal on Wireless Communications and Networking*, vol. 2010, Apr. 2010.

[30] J. Prieto, A. Bahillo, S. Mazuelas, P. Fernández, R. M. Lorenzo, and E. J. Abril, "Self-Calibration of TOA/Distance Relationship for Wireless Localization in Harsh Environments," in *2012 IEEE International Conference on Communications (ICC 2012)*, Jun. 2012.

[31] J. Prieto, A. Bahillo, S. Mazuelas, R. M. Lorenzo, J. Blas, and P. Fernández, "NLOS Mitigation based on Range Estimation Error Characterization in an RTT-based IEEE 802.11 Indoor Location System," in *IEEE International Symposium on Intelligent Signal Processing (WISP 2009)*, Aug. 2009.

[32] Y. Wu, H. Zhang, M. Wu, X. Hu, and D. Hu, "Observability of Strapdown INS Alignment: A Global Perspective," *IEEE Transactions on Aerospace and Electronic Systems*, vol. 48, no. 1, pp. 78–102, Jan. 2012.

[33] A. R. Jiménez, F. Seco, J. C. Prieto, and J. I. Guevara, "Indoor Pedestrian Navigation Using an INS/EKF Framework for Yaw Drift Reduction and a Foot-Mounted IMU," in *7th Workshop on Positioning Navigation and Communication (WPNC)*, Mar. 2010.

[34] S. Julier, J. Uhlmann, and H. F. Durrant-Whyte, "A New Method for the Nonlinear Transformation of Means and Covariances in Filters and Estimators," *IEEE Transactions on Automatic Control*, vol. 45, no. 3, pp. 477–482, Mar. 2000.

APPENDIX

Let $\bar{p} = [p_0, p_1, p_2, p_3]^T \in \mathbb{H}$ and $\bar{q} = [q_0, q_1, q_2, q_3]^T \in \mathbb{H}$ be two quaternions, $p_0 \in \mathbb{R}$ and $q_0 \in \mathbb{R}$ their respective scalar parts, and $\mathbf{p} = [p_1, p_2, p_3]^T \in \mathbb{R}^3$ and $\mathbf{q} = [q_1, q_2, q_3]^T \in \mathbb{R}^3$ their respective vector parts. Their product is defined according to,

$$\bar{p} \odot \bar{q} = \begin{pmatrix} p_0 q_0 - \mathbf{p} \cdot \mathbf{q} \\ p_0 \mathbf{q} + q_0 \mathbf{p} + \mathbf{p} \times \mathbf{q} \end{pmatrix}.$$

The exponential of a quaternion $\bar{q} = [q_0, \mathbf{q}]^T$ is defined as,

$$\exp(\bar{q}) = \exp(q_0) \begin{pmatrix} \cos(\|\mathbf{q}\|) \\ \frac{\mathbf{q}}{\|\mathbf{q}\|} \cos(\|\mathbf{q}\|) \end{pmatrix}.$$

Given a unit quaternion $\bar{q} = [q_0, q_1, q_2, q_3]^T$ representing a rotation, the orthogonal matrix

$$\begin{pmatrix} q_0^2 + q_1^2 - q_2^2 - q_3^2 & 2q_1q_2 - 2q_0q_3 & 2q_1q_3 + 2q_0q_2 \\ 2q_1q_2 + 2q_0q_3 & q_0^2 - q_1^2 + q_2^2 - q_3^2 & 2q_2q_3 - 2q_0q_1 \\ 2q_1q_3 - 2q_0q_2 & 2q_2q_3 + 2q_0q_1 & q_0^2 - q_1^2 - q_2^2 + q_3^2 \end{pmatrix}$$

corresponds to the same rotation.